

Allosteric inhibition of the IRE1 α RNase preserves cell viability and function during endoplasmic reticulum stress

Rajarshi Ghosh, Likun Wang, Eric S. Wang, B. Gayani K. Perera, Aeid Igbaria, Shuhei Morita, Kris Prado, Maike Thamsen, Deborah Caswell, Hector Macias, Kurt F. Weiberth, Micah J. Gliedt, Marcel V. Alavi, Sanjay B. Hari, Arinjay K. Mitra, Barun Bhatarai, Stephan C. Schürer, Erik L. Snapp, Douglas B. Gould, Michael S. German, Bradley J. Backes, Dustin J. Maly, Scott A. Oakes, Feroz R. Papa

SUPPLEMENTAL INFORMATION

SUPPLEMENTAL FIGURE LEGENDS

Figure S1: Irremediable ER stress activates IRE1 α to induce a Terminal UPR and triggers apoptosis. Related to Figure 1

(A) Annexin-V staining of INS-1 cells exposed to increasing [Thapsigargin (Tg)] for up to 72hr. (B) Immunoblot of pro- and cleaved Caspase-3 from Tg-treated INS-1 cells. (C) Percent of INS-1 cells staining positive for Annexin V after treatment with increasing concentrations of Tunicamycin (Tm) for 72hr. (D) Percent of INS-1 cells staining positive for Annexin V after treatment with increasing concentrations of Brefeldin A (BFA) for 72hr. Three independent biological samples were used. Data are plotted as means \pm SD. P-values: * <0.05, **<0.01. (E) Anti-phospho-IRE1 α and anti-total IRE1 α (upper), anti-phospho-JNK and anti-total JNK (lower) immunoblots of INS-1 cells treated for 12hr with increasing concentrations of Tg. GAPDH serves as a loading control. EtBr-stained agarose gel (middle) of XBP1 cDNA amplicons from INS-1 cells treated with increasing concentrations of Tg for 6hr. (F) Quantification of percent XBP1 splicing in same samples in (E). Real-Time PCR (Q-PCR) for Insulin1 and TXNIP mRNA

(normalized to GAPDH) in INS-1 cells treated with increasing concentrations of Tg for 6hr. (G) Percent XBP1 splicing (24hr), relative Insulin1 (Ins1) mRNA levels by Q-PCR (24hr) and percent Annexin V staining (72hr) from 1 μ g/ml doxycycline (Dox) treated INS-1 IRE1 α (I642G) cells +/-1 μ M 1NM-PP1 and +/-6 nM Tg. (H) Percent Annexin V staining (72 hr) of INS-1, INS-1 IRE1 α (I642G), INS-1 IRE1 α (K599A) and INS-1 IRE1 α (N906A) cells exposed to +/- 1 μ g/ml Dox and +/- 6 nM Tg. (I) Anti-Flag-XBP1s immunoblot (left panel) and percent Annexin V staining (right panel) of INS-1:: XBP1s (s=Spliced) cells exposed to +/- 1 μ g/ml Dox for 24hr before exposure to +/- 6 nM Tg. (J) Q-PCR for Insulin1 mRNA (normalized to GAPDH) in 1 μ g/ml Dox -induced INS-1 IRE1 α (I642G) cells treated with Tg (6 nM) and increasing concentrations of 1NM-PP1 for 24hr. (K) Percentage of INS-1 IRE1 α (I642G) cells staining positive for Annexin V after treatment for 72hr with Dox (1 μ g/ml), Tg (6 nM) and increasing concentrations of 1NM-PP1. Three independent biological samples were used for each experiment and plotted as mean value +/- SD. P-values: * <0.05 , ** <0.01 and *** <0.001 , ns=not significant. (L) Immunoblot of Myc-IRE1 α , Pro- and cleaved Caspase-3 from INS-1 IRE1 α (I642G) and INS-1 IRE1 α (I642G/N906A) cells treated for 72hr with combinations of Dox (1 μ g/ml), 1NM-PP1 and Tg. (M) Model of intermediate oligomerization and activation of IRE1 α (I642G) with 1NM-PP1, which is fully sufficient for XBP1 mRNA splicing without ER stress; higher-order oligomerization and extra-XBP1 endonucleolytic decay occurs under irremediable ER stress.

Figure S2: The IRE1 α (Q780 Δ) cancer mutant functions as a dominant negative against XBP1 splicing and apoptotic activities of IRE1 α (WT). Related to Figure 2

(A) RNase activities of recombinant IRE1 α * as measured by the cleavage of the 5'FAM-3'BHQ-labeled XBP1 minisubstrate. Wild type (WT) IRE1 α * was mixed with IRE1 α *(Q780 Δ) or BSA by fixing [WT IRE1 α *] at 0.1 μ M and varying [IRE1 α *(Q780 Δ)] or [BSA] as indicated. (B) EtBr-stained agarose gel of XBP1 cDNA amplicons from INS-1 IRE1 α human (WT) and human IRE1 α (Q780 Δ) stable cells treated with 1 μ g/ml Dox for 24hr prior to treatment with 100 ng/ml Tm for 8hr. (C) Quantification of percent XBP1 splicing from (B). (D) Percent of INS-1 human IRE1 α (Q780 Δ) stable cells staining positive for Annexin V after Dox (1 μ g/ml) for 48hr followed by treatment with 50 ng/ml Tm for 72hr. Three independent biological samples were used for Annexin V staining experiments. Data are plotted as means +/- SD. p-values: * <0.05, **<0.01.

Figure S3: sfGFP-IRE1 α reporter exhibits pro-apoptotic features of IRE1 α and sfGFP-IRE1 α (I642G) demonstrates graded oligomerization states. Related to Figure 3

(A) Model of N-terminal sfGFP-IRE1 α and Kinase/RNase linker IRE1 α -3F6HGFP reporter (top panel). EtBr-stained agarose gel of XBP1 cDNA amplicons from INS-1 sfGFP-IRE1 α and INS-1 IRE1 α -3F6HGFP isogenic stable cells treated with 1 μ g/mL Dox for indicated times (center panel). Lower panel shows quantification of percent XBP1 splicing above. (B) Percentage of Annexin V positive INS-1 sfGFP-IRE1 α and IRE1 α -3F6HGFP stable cells treated with 1 μ g/mL Dox for 96hr. Three independent biological samples were used for Annexin V staining experiments. Data are plotted as means +/- SD. p-values: **<0.01, ns= not significant. (C) Model of N-terminal sfGFP-IRE1 α (I642G) reporter (top panel). Images show sfGFP-IRE1 α (I642G) induced with 1 ng/ml Dox for 12hr in INS-1 cells +/- DTT (5 mM) for 20 min either in the presence or absence of 1NM-PP1 (5 μ M). Scale bar is 5 μ m. (D) EtBr-stained agarose gel of

XBP1 cDNA amplicons from INS-1 sfGFP-IRE1 α (I642G) stable cells treated with 1 μ g/ml Dox for indicated times (center panel). Lower panel shows quantification of % XBP1 splicing above.

Figure S4: KIRA6 and 1NM-PP1 have opposing effects on IRE1 α (I642G). Related to Figure 4

(A) MTT assay of INS-1 cells treated with increasing concentration of APY29 (left panel) and KIRA6 (right panel) for indicated timepoints. Data are shown from 3 biological replicates and plotted as means \pm SD. (B) Q-PCR for Insulin1 (Ins1) mRNA (normalized to GAPDH) in Dox treated INS-1 IRE1 α (I642G) cells treated with Tm (0.5 μ g/ml) and increasing concentrations of 1NM-PP1 in the presence or absence of KIRA6 (1 μ M) for 24hr. (C) Percentage of INS-1 IRE1 α (I642G) cells staining positive for Annexin V after treatment for 72hr with Dox (1 μ g/ml), Tm (0.5 μ g/ml), and increasing concentrations of 1NM-PP1 in the presence or absence of KIRA6 (1 μ M). Data are from 3 biological replicates and plotted as means \pm SD. p-values: * $<$ 0.05, ** $<$ 0.01. (D) Table showing IC₅₀ values of kinase inhibitory activity of KIRA6 against a panel of 7 indicated kinases *in vitro*. (E) Immunoblots for phospho-eIF2 α and total eIF2 α , phospho-IRE1 α and total IRE1 α in INS-1 cells pretreated for 1hr with indicated concentrations of KIRA6, followed by treatment with Tg (1 μ M) for 2hr. GAPDH serves as a loading control.

Figure S5: KIRA6 inhibits Terminal UPR outputs of IRE1 α to protect against ER stress-induced apoptosis. Related to Figure 5

(A) Structure of (NMe)KIRA6. (B) RNase activity of IRE1 α * in the presence or absence of (NMe)KIRA6 (20 μ M) as measured by the cleavage of the 5'FAM-3'BHQ-labeled XBP1 minisubstrate. (C) Q-PCR for Insulin2 (Ins2) mRNA in INS-1 cells 12hr after Tm (0.5 μ g/ml) in

cells pre-treated for 1hr with indicated [KIRA6]. (D) IRE1 α induction of miR-17 binding dependent TXNIP reporter is attenuated by KIRA6. Dox-inducible INS-1 IRE1 α (WT) cells were transfected with a luciferase reporter construct containing TXNIP 3' UTR. The cells were treated with or without 100 ng/ml Dox for 24hr, lysed and then analyzed for luciferase activity. Three independent biological samples were used for luciferase experiments. Data are shown as mean +/- SD. *p < 0.05 ;**p < 0.01;***p < 0.005. (E) Immunofluorescence staining of EdU (green) and β -cell nuclear marker, Nkx6.1(red), in C57BL/6 mouse islets treated with 0.5 μ g/ml Tm +/-0.5 μ M KIRA6 for 48hr. White color shows the co-localization of the red and green channels. (F) Immunofluorescence staining of healthy non-diabetic human islets treated with 0.5 μ g/mL Tm +/-0.5 μ M KIRA6 for 16hr as indicated. Co-stained for DAPI (blue), insulin (green), and TUNEL (red). Merged image is also shown. Lower panel shows quantification of TUNEL positive β -cells (white arrows) normalized to DAPI-positive cells. (G) Structure of STF-083010 and cartoon showing that it directly inhibits the RNase of IRE1 α (through covalent modification). (H) Q-PCR for Ins1 mRNA in INS-1 IRE1 α (WT) cells treated with Dox (5 ng/ml) +/- STF-083010 (50 μ M) over the indicated timecourse. (I) Annexin V staining of INS-1 cells after 72hr with indicated [Tm] +/- STF-083010 (50 μ M). (J) Annexin V staining of INS-1 cells after 72hr with Tm (0.2 μ g/ml), STF-083010 (1 or 5 μ M), and KIRA6 (0.05 μ M) as indicated. Data plotted as mean +/- SD. P-values: *<0.05, ** <0.01, *** <0.005.

Figure S6: KIRA6 protects against cell degeneration and death in rodent model of ER stress-induced retinal degeneration. Related to Figure 6

(A-B) Histological sections of retinas from P23H rats (asterisks indicate outer nuclear layer (ONL)) and quantification of ONL thickness (n=4) of P23H and Sprague-Dawley (SD) rats.

P23H rats were injected with 10 μ M KIRA6 or DMSO at P9 and P15 and analyzed at P40. (C) Urea PAGE of cleavage reactions of 32 P-labeled Rhodopsin mRNA by IRE1 α *(WT) or the RNase-dead mutant, IRE1 α *(N906A), incubated with indicated doses of KIRA6. Black arrow indicates intact RNA and red arrows indicate cleavage products. (D) Representative ERG recordings of wild-type SD rats that were intravitreally injected with 2 μ l Tm (n=10), Tm + KIRA6 (n=7) or an equivalent amount of DMSO (n=3) to achieve a final concentration of 3 μ g/ml Tm and 10 μ M KIRA6 in the vitreous at P21; ERG measurements at a light intensity of 0 dB were recorded at P28.

Figure S7: Systemic KIRA6 reduces Terminal UPR endpoints and protects against cell degeneration and death in the Akita diabetic mouse. Related to Figure 7

(A-D) XBP1 splicing (A,C) and Blos1 mRNA levels (B,D) were measured in livers of 8 week-old male C57BL/6 mice. Mice were injected with KIRA6 (25 mg/kg) intraperitoneally twice with an 8hr interval. After 4hr of first KIRA6 dose, the animals were injected with Tunicamycin (2 μ g/kg) (A,B) or (100 μ g/kg) (C,D). Animals were sacrificed 12hr after first KIRA6 injection and their livers were harvested for RNA collection. Averages from 3 biological replicates with $n = 3$. Data are plotted as mean \pm SEM. P-values: * <0.05 , ** <0.01 , *** <0.001 . (E) Random blood glucose measurement of male *Ins2*^{+/*Akita*} mice injected with either KIRA6 (10 mg/kg body weight)(n=4) or vehicle (n=6) b.i.d. starting at 3 weeks of age. Injections were stopped after 33 days. BGs (mean \pm SEM) also analyzed for significance by Two-way RM ANOVA; p-value = 0.0145. (F) Total body weight of the mice in (K) at day 49. Data are plotted as means \pm SD. p-values: * <0.05 , ** <0.01 . (G) TXNIP mRNA levels were measured in islets of male *Ins2*^{+/*Akita*} mice injected with either KIRA6 (5 mg/kg body weight)(n=3) or vehicle (n=2) b.i.d. starting at 3

weeks age. Injections were continued for 7 days after which islets were harvested. (H) CHOP mRNA levels of the same samples as in (G). Data are plotted as means +/- SD. p-values: * <0.05 .

SUPPLEMENTAL MOVIE LEGENDS

Movies S3(A-F): IRE1 α apoptotic outputs are blocked in mutant cell lines. Related to Figure 3

Time lapsed video of INS-1 hIRE1 α (WT), (Q780*) and (P830L) stable cells (pictures taken at 30 min intervals) treated with (Movies S3A, B, C, respectively) or without Dox (1 μ g/ml) (Movies S3D, E, F respectively) for 72hr under inverted bright-field microscope.

Movies S5(A-C): KIRA6 allows cell proliferation under ER stress. Related to Figure 5

Time-lapsed microscopy (pictures taken at 30 min intervals) of INS-1 cells, untreated (Movie S5A), treated with Tm (0.5 μ g/ml) (Movie S5B) or Tm (0.5 μ g/ml) plus KIRA6 (0.5 μ M) (Movie S5C) for 72hr under inverted bright-field microscope.

SUPPLEMENTAL EXPERIMENTAL PROCEDURES

Tissue Culture

INS-1 cells with doxycycline (Dox)-inducible expression of wild-type and mutant mouse IRE1 α were grown in RPMI, 10% fetal bovine serum, 1 mM sodium pyruvate, 10 mM HEPES, 2 mM glutamine, 50 μ M β -mercaptoethanol, as described previously (Han *et al.*, 2009). To generate the Dox-inducible IRE1 α human (WT) and IRE1 α human cancer mutant cell lines, INS-1/FRT/TO cells were grown in the above media with 10 μ g/ml blasticidin. Cells were then grown in 200 μ g/ml zeocin, cotransfected with 1 μ g pcDNA5/FRT/TO:IRE1 α human (WT), (L474R),

(R635W), (S769F), (Q780*) and (P830L) mutant constructs and 1 μ g FLP recombinase (pOG44) using Lipofectamine (Invitrogen). After 4hr, cells were switched to zeocin-free media, trypsinized 48hr later, and then plated in media containing hygromycin (150 μ g/ml), which was replaced every 3 days until colonies appeared. Thapsigargin (Tg), Brefeldin A (BFA), and Dox were purchased from Sigma-Aldrich. Tunicamycin (Tm) was purchased from Millipore. APY29, KIRA6, 1NM-PP1 and (NMe)KIRA6 were synthesized in house.

Western Blots and Antibodies

For protein analysis, cells were lysed in M-PER buffer (Thermo Scientific) plus complete EDTA-free protease inhibitor (Roche) and phosphatase inhibitor cocktail (Sigma). The concentration of samples was determined using BCA Protein Assay (Thermo). Western blots were performed using 10% and 12% Bis-Tris precast gels (NuPage) on Invitrogen XCell SureLock® Mini-Cell modules. Gels were run using MES buffer and transferred onto nitrocellulose transfer membrane using an XCell II™ Blot Module. Blocking, antibody incubation, and washing were done in PBS or TBS with 0.05% Tween-20 (v/v) and 5% (w/v) non-fat dry milk or BSA, or blocking buffer (Licor-Odyssey). Antibodies used were: mouse anti-Actin (Sigma-Aldrich); rabbit anti-cleaved Caspase-2 (Abcam); mouse anti-GAPDH, anti-c-Myc, anti-rabbit, anti-proinsulin, and anti-IRE1 α (Santa Cruz Biotechnology); anti-phospho-IRE1 α and anti-full length Caspase-2 (Novus Biologicals); and rabbit anti-Caspase-3, anti-JNK, anti-eIF2 α , anti-phospho-eIF2 α , and mouse anti-phospho-JNK (Cell Signaling). Antibody binding was detected by using near-infrared-dye-conjugated secondary antibodies (Licor) on the LI-COR Odyssey scanner or visualized by capturing on a CL-XPosure film using ECL SuperSignal West Dura Extended Duration Substrate (both from Thermo Scientific).

RNA isolation, Real-Time PCR (Q-PCR), and Primers

RNA was isolated from whole cells using either Qiagen RNeasy kits or Trizol (Invitrogen). TissueLyser II (Qiagen) was used for RNA isolation from liver and retina. Primers used for Q-PCR were as follows: Rat TXNIP: 5'-CTGATGGAGGCACAGTGAGA-3' and 5'-CTCGGGTGGAGTGCTTAGAG-3'; rat GAPDH 5'-AGTTCAACGGCACAGTCAAG-3' and 5'-ACTCAGCACCAGCATCACC-3'; rat Ins1, 5'-GTCCTCTGGGAGCCCAAG-3' and 5'-ACAGAGCCTCCACCAGG-3'; rat Ins2, 5'-ATCCTCTGGGAGCCCCGC-3' and 5'-AGAGAGCTTCCACCAAG-3'; rat p21, 5'-TGAACCGCTGTCTTGAGATG-3' and 5'-TCTTGGTTGCCTCTTTTGCT-3'; mouse Blos1, 5'-CAAGGAGCTGCAGGAGAAGA-3' and 5'-GCCTGGTTGAAGTTCTCCAC-3'; mouse Beta-Actin, 5'-GCAAGTGCTTCTAGGCGGAC-3' and 5'-AAGAAAGGGTGTAACACGCAGC-3'. For standard mRNA, 1 µg total RNA was reverse transcribed using the QuantiTect Reverse Transcription Kit (Qiagen). For Q-PCR, we used SYBR green (Qiagen) and StepOnePlus Real-Time PCR System (Applied Biosystems). Thermal cycles were: 5 min at 95 °C, 40 cycles of 15 s at 95 °C, 30 s at 60 °C. Gene expression levels were normalized to GAPDH or Actin.

For TaqMan Q-PCR, cDNA was produced using a target-specific probe, TaqMan Universal PCR Master Mix, the TaqMan microRNA reverse transcription kit (both Applied Biosystems) and the Bio-Rad iCycler Thermal cycler. For both regular Q-PCR and TaqMan Q-PCR, the reactions were performed on C1000 thermal cycler and measurements were recorded on a CFX96 Real-Time PCR Detection System (both from Bio-Rad). The following targeted primers and probes sets were used in TaqMan Q-PCR: snoRNA135, RPL21 and hsa-miR-17 (all from Applied Biosystems).

XBP-1 mRNA splicing

RNA was isolated from whole cells or tissues and reverse transcribed as above to obtain total cDNA. Then, XBP-1 primers were used to amplify an XBP-1 amplicon spanning the 26 nt intron from the cDNA samples in a regular 3-step PCR. Thermal cycles were: 5 min at 95 °C, 30 cycles of 30 s at 95 °C, 30 s at 60 °C, and 1 min at 72 °C, followed by 72 °C for 15 min, and a 4 °C hold. Sense primer rat XBP1.3S (5'-AAACAGAGTAGCACAGACTGC-3') and antisense primer rat XBP1.2AS (5'-GGATCTCTAAGACTAGAGGCTTGGTG-3') were used. PCR fragments were then digested by PstI, resolved on 2% agarose gels, stained with EtBr and quantified by densitometry using ImageJ (U. S. National Institutes of Health). Spliced XBP1 was also determined in mouse liver by Q-PCR using mouse XBP1 sense (5'-AGGAAACTGAAAAACAGAGTAGCAGC-3') and antisense (5'-TCCTTCTGGGTAGACCTCTGG-3') primers.

Flow Cytometry

For assaying apoptosis by Annexin V staining, cells were plated in 12-well plates overnight. Cells were then treated with various reagents for indicated time periods. On the day of flow cytometry analysis, cells were trypsinized and washed in PBS and resuspended in Annexin V binding buffer with Annexin-V FITC (BD Pharmingen™). Flow cytometry was performed on a Becton Dickinson LSRII flow cytometer.

Islet staining

Islets were extracted from C57BL/6 mice using previously reported methods (Szot et al., 2007), and cultured in RPMI + 10% FBS with 0.5 µg/mL Tm with or without KIRA6 (0.5 µM) or left untreated for 16hr. Approximately 150 islets were cultured for each condition in triplicate. Non-

diabetic human islets were obtained from Prodo Labs (Irvine, CA) and cultured in Prodo Islet Medium (PIM from Prodo Labs). For analysis of non-ER stress treated conditions, islets were cultured in PIM for 16hr before harvesting. Islets were then spun, washed once with PBS, and fixed for 30 min with 4% PFA. After fixation, islets were washed twice with PBS, followed by a wash in 100% ethanol. After removal of all ethanol, 100 μ l of prewarmed Histogel (Thermo Scientific) was added to the eppendorf tube and placed at 4°C to solidify before paraffin embedding and 5 μ m sectioning of the islets. Islets were stained with TUNEL using ApopTag® Red In Situ Apoptosis Detection Kit (Millipore) according to the manufacturer's instructions. Islets were also co-stained with anti-TXNIP (MBL International), guinea pig anti-insulin (Zymed), DAPI (Sigma), and goat anti-guinea pig secondary (Rockland) before mounting onto slides with VectaShield (Vector Laboratories). At least 10 islets and > 500 β -cell nuclei were counted per group, in triplicate. Cells were considered TUNEL positive if staining was present and colocalized with DAPI staining, indicating nuclear localization.

MTT assay

INS-1 CAT, IRE1 α human (WT) and IRE1 α human mutant cells were seeded at 40% confluence in a 96-well plate and treated or not treated with indicated concentrations of Tg or Dox (1 μ g/ml). At the indicated time points, medium was replaced with 100 μ l of 1 mg/ml 3-(4,5-dimethylthiazol-2-yl)-2,5-diphenyltetrazolium bromide (MTT) (Molecular Probes) in RPMI. After incubation at 37°C for 4hr, 75 μ l MTT medium was removed, and 50 μ l DMSO were added to dissolve precipitate. Absorbance was recorded at 540 nm using a Spectramax M5 microplate reader (Molecular Devices).

Superfolder GFP-IRE1 α construction and microscopy

The first 27 amino acids of mouse IRE1 α containing the signal peptide were cloned just before the first ATG of sfGFP lacking the stop codon, and the rest of the sequence of mouse IRE1 α (WT) or IRE1 α (I642G) was cloned in frame after the sfGFP in a pCDNA5 FRT/TO mammalian expression plasmid. INS1- FRT/TO cells were transfected as described previously (Han *et al.*, 2009) to generate stable cell lines expressing the above constructs, as well as the previously described reporter, IRE1-3F6HGFP that contains an EGFP domain positioned close to the kinase (Li et al., 2010). After induction of INS1-sfGFP-IRE1 α cells for 24hr with 1 ng/ml Dox (a sub-apoptotic dose sufficient for imaging the reporter), live cells were imaged on a widefield microscope after a further treatment with 1 mM DTT in the presence or absence of 1 μ M KIRA6 (Axiovert 200; Carl Zeiss MicroImaging, Inc.) with a 63X/1.4 NA oil objective and a 450-490nm excitation/500-550 emission bandpass filter using a Retiga 2000R camera. Composite figures were prepared using ImageJ (NIH), Photoshop CS4 and Illustrator CS4 software (Adobe). For INS1-sfGFP-IRE1 α (I642G) cells, 5 μ M 1NM-PP1 was used for induction in presence of 1 ng/ml Dox for 12hr. Live cells were imaged (Nikon Eclipse Ti-Yokogawa CSU22 spinning disk confocal) with Apo 100X/1.49 oil objective and a 491nm excitation/525-50 emission filter. Figures were prepared using ImageJ (NIH).

Null Hong Kong α -1 Antitrypsin De-glycosylation immunoblots

pCDNA3.1- α 1 hAT-NHK plasmid expressing the NHK- α 1AT, a kind gift of Rick Siefers (Baylor College of Medicine) was transfected into HEK293 cells. Cells were then treated with Tm +/- KIRA6 to check protein glycosylation status. NHK- α 1AT remains glycosylated under normal conditions producing a protein band at \sim 50 kDa by immunoblot. However, Tm treatment inhibits glycosylation and the deglycosylated band appears at \sim 42 kDa. Goat anti-human α 1-

antitrypsin antibody (MP biomedical) was used for detection by immunoblot.

Detection of IL1- β

Human THP-1 cells were grown in RPMI-1640 with 10% FBS and 50 μ M 2-mercaptoethanol, differentiated for 2hr with 0.5 μ M phorbol-12-myristate-13-acetate (Sigma), and primed for 18hr with 1 μ g/ml ultrapure lipopolysaccharide (LPS; Sigma). Cell culture media was changed to media without LPS and treated with 0.5 μ M KIRA6 for 2hr prior to the addition of 5 mM ATP (Roche), or 1 μ M Tg or 10 μ g/ml Tm. After 4hr incubation, media supernatant was collected and assayed for hIL-1 β by ELISA (Thermo Scientific).

TXNIP 3'UTR Reporter Luciferase Assay

Luciferase reporter containing TXNIP 3' UTR with miR-17 binding sites was used as described (Lerner et al., 2012). To measure luciferase activity a Dual-Glo (Promega #E2920) kit was used as per manufacturer's instructions. The luciferase enzyme activity was detected on a Spectramax M5 microplate reader (Molecular Devices).

Glucose-stimulated insulin secretion (GSIS) assay

Freshly isolated islets from 9-week-old C57BL/6 mice were cultured in RPMI-1640 with 10% FCS, 2 mM L-glutamine, 0.1 mM 2-mercaptoethanol, and 11 mM glucose with or without Tm (500 ng/ml) for 16hr before the GSIS assay. KIRA6 (0.5 μ M) was added 2hr before treating with Tm. In the GSIS assay, islets were preincubated in HEPES-buffered Krebs-Ringer bicarbonate solution (KRBH) (10 mM HEPES [pH 7.4], 129 mM NaCl, 4.7 mM KCl, 1.2 mM KH₂PO₄, 1.2 mM MgSO₄, 2 mM CaCl₂, 5 mM NaHCO₃, and 0.1% BSA) containing 2.5 mM glucose for 30 min at 37° C. Thirty islets per condition were incubated with either 2.5 mM or 16.7 mM glucose

in KRBH at 37°C for 60 min. Collected media were analyzed by anti-insulin ELISA (EMD Millipore).

Intravitreal Injections of small molecules

2 µl was injected intravitreally into each eye to achieve the indicated final concentrations based on known rat vitreous volumes. Tm (20 µg/µl final concentration) +/- KIRA6 (10 µM final concentration) was injected into SD rats at P21 with an equivalent amount of DMSO as a vehicle control. Retinas were collected at 72 and 96hr after injections in Trizol (Invitrogen) for Q-PCR analysis. Eyes were examined by optical coherence tomography (OCT) 7 days post injection and subsequently collected for morphological analysis. P23H rats were injected with KIRA6 (10 µM final concentration) or DMSO vehicle control at P9 and P15, and eyes were examined at P40 by OCT and by morphological analysis.

Image guided optical coherence tomography (OCT)

Mice were anaesthetized with 1.5-3% isoflurane, eyes were dilated with 2.5% phenylephrine hydrochloride and 1% tropicamide, and corneas were kept moist with regular application of 2.5% methylcellulose. Eyes were examined using a Micron III retinal imaging system (Phoenix Research Labs). Spectral domain OCT images were acquired with a Micron Image Guided OCT System (Phoenix Research Labs) by averaging 10 to 50 scans.

Morphological analysis of retinas

Outer nuclear layers (ONL) were quantified as previously described (Lewin et al., 1998). Briefly, rats were euthanized by CO₂ inhalation and their eyes were immediately enucleated and immersed in 2% paraformaldehyde and 2.5% glutaraldehyde in phosphate buffered saline.

Subsequently, eyes were bisected on the vertical meridian through the optic nerve head and embedded in Epon-Araldite resin; 1 μm sections were cut and stained with toluidine blue. ONL thickness was measured at 54 locations around the retina using Bioquant image analysis (Bioquant; R&M Biometrics).

Electroretinography (ERG)

Rats dark-adapted overnight were anesthetized with ketamine (87 mg/kg) and xylazine (13 mg/kg) via i.p. injection in dim red light. Pupils were dilated with 2.5% phenylephrine hydrochloride and 1.0% tropicamide, and corneas were anesthetized with 0.5% proparacaine. Scotopic ERG recordings were performed as previously described (McGill et al., 2007). Briefly, 10- μsec flashes of white light of increasing intensities were used to induce bilateral, full-field ERGs; responses were recorded using contact lens electrodes with a UTAS-E 3000 Visual Electrodiagnostic System (LKC Technologies, Inc.). *Electroretinography (ERG)*

Islet culture and proliferation assessment (EdU staining)

C57BL/6 mouse islets were isolated as previously described (Szot et al., 2007), cultured for 5 days, followed by 2 days of indicated treatment. DMSO was utilized as control, Tm at 0.5 $\mu\text{g/ml}$, and KIRA6 at 1 μM . After 48hr, islets were treated with 10 mM 5-Ethynyl-2-deoxyuridine (EdU) for 3hr, and then immediately fixed in 4% paraformaldehyde/10 mM PBS solution for 25 min. Islets were washed 3 times with 10 mM PBS for 20 min, permeabilized with 0.3% TritonX-100 in 10 mM PBS for 3hr, then blocked in 5% goat serum/0.15% Triton-X 100/10 mM PBS overnight at 4°C and washed twice with antibody dilution buffer for 15 min at room temperature. Primary antibody, rabbit anti-human NKX6.1 1:500 (Sigma-Aldrich), and secondary antibody, Cy3 conjugated goat anti-rabbit 1:500 (Sigma), were diluted in 1% BSA/0.2% Triton X-100/10

mM PBS and incubated for 24hr at 4°C. Click-iT® EdU Alexa Fluor® Imaging Kit (Invitrogen) was used to identify dividing cells after immunostaining. Islets were mounted with Fluoromount™ (Sigma) and imaged using a Leica SP5 confocal laser scanning microscope (Leica). The Volocity software (PerkinElmer) colocalization macro was utilized to quantify dual EdU and the unique β-cell nuclear marker Nkx6.1.

Animal analytic studies

C567BL/6 and C57BL/6 $Ins2^{WT/C96Y}$ ($Ins2^{+/Akita}$) mice were obtained from Jackson Laboratories. Glucose levels were measured from tail snips obtained between 9:00 and 11:00 AM using a glucometer (Nova Statstrip Xpress, Data Sciences International). Serum insulin and C-peptide levels were measured using mouse ultra-sensitive insulin and C-peptide ELISA (Merckodia). All procedures described involving animals were performed in accordance with protocols approved by the Institutional Animal Care and Use Committee at the University of California, San Francisco. Animals were maintained in a specific pathogen-free animal facility on a 12hr light–dark cycle at an ambient temperature of 21°C. They were given free access to water and food. All experiments used age-matched male mice.

$Ins2^{+/Akita}$ mouse genotyping

Akita mouse colonies were maintained and genotyped as described previously (Lerner et al., 2012).

Glucose Tolerance Test

Mice were fasted for 17hr before i.p. injection with glucose (2 g/kg). Blood was collected from the tail, and glucose levels were determined using a glucometer (Nova Statstrip Xpress, Data Sciences International).

Mouse injections

Male *Ins2^{+/-Akita}* mice were injected i.p. with KIRA6 in a 2 mg/ml solution made of 3% Ethanol: 7% Tween-80: 90% Saline twice a day (b.i.d). Same solution without KIRA6 is denoted as Vehicle. C567BL/6 mice were also injected with same KIRA6 solution and indicated doses of Tm for liver analysis.

Pancreatic Insulin-positive β -cell area determination

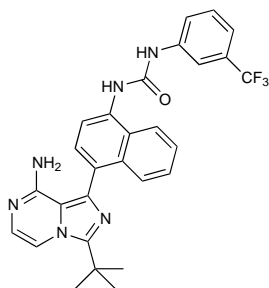
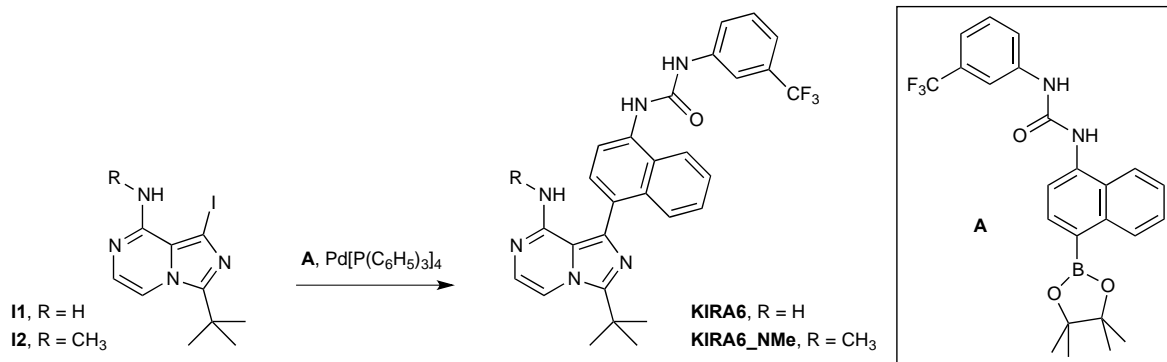
Pancreatic sectioning, staining and analysis were done as described previously (Chintinne et al., 2010). Briefly, whole pancreas in paraffin-embedded blocks from vehicle (n=3) and KIRA6 (n=6) treated mice were serially sectioned at intervals of 250 μ m. Every 10th section was stained with anti-insulin (Invitrogen). Nuclei were stained with DAPI (Sigma-Aldrich). A minimum of 2% of the total organ volume was stained and measured. The pancreas and β -cell areas were measured with the Zeiss AxioImager Brightfield Microscope and quantified with VOLOCITY software.

Rat husbandry

All studies and procedures were performed in accordance with the guidelines of the Institutional Animal Care and Use Committee at the University of California, San Francisco, and in compliance with the ARVO Statement for the Use of Animals in Ophthalmic and Vision Research. P23H rhodopsin transgenic rats (line 1) were described previously

(<http://www.ucsfeye.net/mlavailRDratmodels.shtml>); wild-type Sprague-Dawley (SD) rats served as controls. All animals were housed in barrier facility free of specific pathogens on a 12hr light/dark cycle with food and water available *ad libitum*.

KIRA6 and KIRA6_NMe synthesis.



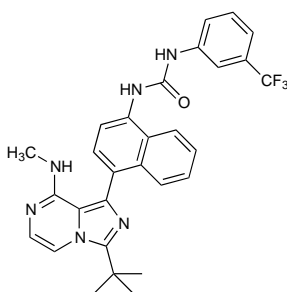
KIRA6

1-(4-(8-amino-3-tert-butylimidazo[1,5-a]pyrazin-1-yl)naphthalen-1-yl)-3-(3-

(trifluoromethyl)phenyl)urea (KIRA6). A mixture of **I1** (60.0 mg, 0.120 mmol), **A** (66 mg, 0.15

mmol), tetrakis(triphenylphosphine)palladium (5 mg, 4 μ mol) and sodium carbonate (928 mg, 0.27 mmol) was dissolved in a 3:1 mixture of DME/water (0.5 ml). The mixture was heated overnight at 85°C. The crude mixture was cooled to room temperature, diluted in a mixture of acetonitrile/water and purified by reverse phase chromatography (HPLC) to obtain 53 mg of KIRA6. TLC (CH₂Cl₂:MeOH, 95:5 v/v): R_f = 0.4; ¹H NMR (300 MHz, MeOD): δ 8.26 (m, 1H), 8.08-7.99 (m, 2H), 7.90-7.86 (m, 1H), 7.83-7.79 (m, 1H), 7.69- 7.52 (m, 5H), 7.35 (d, *J* = 7.4 Hz, 1H), 6.98 (m, 1H), 1.65 (s, 9H); ¹³C NMR (126 MHz, MeOD): δ 154.8, 140.2, 135.7, 133.0, 132.4, 131.7, 131.6, 131.0, 130.7, 129.4, 128.8, 128.6, 128.5, 127.0, 126.6, 125.9, 125.4, 123.2, 121.9, 120.1, 118.7, 115.0, 114.4, 110.1, 33.6, 27.3; ESI-MS (m/z): [M]⁺ calcd. for C₂₈H₂₅F₃N₆O (M+H⁺): 519.2; found 519.4.

The purity of KIRA6 was determined with two analytical RP-HPLC methods, using a Varian Microsorb-MV 100-5 C18 column (4.6 mm x 150 mm), and eluted with either H₂O/CH₃CN or H₂O/ MeOH gradient solvent systems (+0.05% TFA) run over 30 min. Products were detected by UV at 254 nm. KIRA6 was found to be >95% pure in both solvent systems.



(NMe)KIRA6

1-(4-(8-methylamino-3-tert-butylimidazo[1,5-a]pyrazin-1-yl)naphthalen-1-yl)-3-(3-(trifluoromethyl)phenyl)urea ((NMe)KIRA6). A mixture of **I2** (14.6 mg, 0.044 mmol), **A** (22 mg, 0.048 mmol), tetrakis(triphenylphosphine)palladium (2.0 mg, 1.73 μ mol) and sodium

carbonate (13.6 mg, 0.128 mmol) was dissolved in a 3:1 mixture of DME/water (0.22 ml). The mixture was heated overnight at 85°C. The crude mixture was cooled to room temperature, diluted in a mixture of acetonitrile/water and purified by reverse phase chromatography (HPLC) to obtain 10.2 mg of (NMe)KIRA6. TLC (CH₂Cl₂:MeOH, 95:5 v/v): R_f = 0.4; ¹H NMR (300 MHz, Chloroform-d) δ 9.06 (m, 1H) , 8.63 (m, 1H) , 8.19 (d, *J* = 6.7 Hz, 1H), 8.05 (m, 1H), 7.68 (s, 1H), 7.56 – 7.46 (m, 3H), 7.18 (m, 3H), 7.01 – 6.95 (m, 1H), 3.08 (s, 3H), 1.58 (s, 9H); ESI-MS (m/z): [M]⁺ calcd. for C₂₉H₂₇F₃N₆O (M+H⁺): 533.2; found 533.6.

The purity of (NMe)KIRA6 was determined with two analytical RP-HPLC methods, using a Varian Microsorb-MV 100-5 C18 column (4.6 mm x 150 mm), and eluted with either H₂O/CH₃CN or H₂O/ MeOH gradient solvent systems (+0.05% TFA) run over 30 min. Products were detected by UV at 254 nm. (NMe)KIRA6 was found to be >95% pure in both solvent systems.

In vitro IRE1α* protein preparation, crosslinking, RNase and kinase assay.

A construct containing the cytosolic kinase and RNase domains of human IRE1α (residues 469-977, IRE1α*) or equivalent IRE1α mutants was expressed in SF9 insect cells using the Bac-to-Bac baculovirus expression system (Invitrogen) as described (Wang et al., 2012). λ-PPase (NEB)-treated dephosphorylated IRE1α* (dP-IRE1α*) was also prepared and all the crosslinking experiments were performed as described (Wang et al., 2012). The RNase assay using 5'FAM-3'BHQ-labeled XBP1 single stem-loop minisubstrate (5'FAM-CUGAGUCCGCAGCACUCAG-3'BHQ, from Dharmacon), and the IRE1α* auto-phosphorylation kinase assay were both done as described (Wang et al., 2012). The ability of

KIRA6 to inhibit the catalytic activity of Erk2, JNK2, JNK3, PKA, and Pim1 was determined using previously reported assay conditions (Hill *et al.*, 2012). Internally ³²P-labeled RNAs (mouse XBP1 RNA and Ins2 RNA, as described in (Han et al., 2009), and rat rhodopsin mRNA) were also used as substrates. For time-course determination, IRE1 α^* proteins (16 nM) were incubated with or without 10 μ M 1NM-PP1 for 20 min prior to addition of 20 nM radio-labeled RNAs. Reactions were quenched by addition of 4 M urea at different time points and then were subjected to urea 6% PAGE analysis. For the endpoint readings of APY29-mediated rescue of IRE1 α^* P830L RNase activity, IRE1 α^* (WT or P830L) was incubated with 20 μ M APY29 and mixed with 3 μ M XBP1 minisubstrate for 10 min reaction and subsequently resolved by urea 15% PAGE (Wang et al., 2012). Determination of KIRA6-mediated inhibition of WT IRE1 α^* was done by incubating 100 nM IRE1 α^* with the mixture of 3 μ M XBP1 minisubstrate and 220 nM radio-labeled mouse Ins2 RNA, or 150 nM IRE1 α^* and 20 nM radio-labeled rat rhodopsin mRNA. The cleavage buffer and general manipulation are the same as described (Wang et al., 2012). cDNA for rat rhodopsin was purchased from Invitrogen and amplified by PCR using primers: 5'-GAAATTAATACGACTCACTATAGGGGGTCCAGGTACATCCCCGAG-3' (forward) and 5'-TTAGGCTGGAGCCACCTGGCT-3' (reverse). RNA was *in vitro* transcribed, cleaved by IRE1 α^* , and the cleavage sites mapped as described (Wang et al., 2012).

REFERENCES

- Chintinne, M., Stange, G., Denys, B., In 't Veld, P., Hellemans, K., Pipeleers-Marichal, M., Ling, Z., and Pipeleers, D. (2010). Contribution of postnatally formed small beta cell aggregates to functional beta cell mass in adult rat pancreas. *Diabetologia* 53, 2380-2388.
- Han, D., Lerner, A.G., Vande Walle, L., Upton, J.P., Xu, W., Hagen, A., Backes, B.J., Oakes, S.A., and Papa, F.R. (2009). IRE1alpha kinase activation modes control alternate endoribonuclease outputs to determine divergent cell fates. *Cell* 138, 562-575.
- Lerner, A.G., Upton, J.P., Praveen, P.V., Ghosh, R., Nakagawa, Y., Igarria, A., Shen, S., Nguyen, V., Backes, B.J., Heiman, M., *et al.* (2012). IRE1alpha induces thioredoxin-interacting protein to activate the NLRP3 inflammasome and promote programmed cell death under irremediable ER stress. *Cell Metab* 16, 250-264.

Lewin, A.S., Drenser, K.A., Hauswirth, W.W., Nishikawa, S., Yasumura, D., Flannery, J.G., and LaVail, M.M. (1998). Ribozyme rescue of photoreceptor cells in a transgenic rat model of autosomal dominant retinitis pigmentosa. *Nature medicine* 4, 967-971.

Li, H., Korennykh, A.V., Behrman, S.L., and Walter, P. (2010). Mammalian endoplasmic reticulum stress sensor IRE1 signals by dynamic clustering. *Proc Natl Acad Sci U S A* 107, 16113-16118.

McGill, T.J., Prusky, G.T., Douglas, R.M., Yasumura, D., Matthes, M.T., Nune, G., Donohue-Rolfe, K., Yang, H., Niculescu, D., Hauswirth, W.W., *et al.* (2007). Intraocular CNTF reduces vision in normal rats in a dose-dependent manner. *Invest Ophthalmol Vis Sci* 48, 5756-5766.

Szot, G.L., Koudria, P., and Bluestone, J.A. (2007). Murine pancreatic islet isolation. *J Vis Exp*, 255.

Wang, L., Perera, B.G., Hari, S.B., Bhatarai, B., Backes, B.J., Seeliger, M.A., Schurer, S.C., Oakes, S.A., Papa, F.R., and Maly, D.J. (2012). Divergent allosteric control of the IRE1alpha endoribonuclease using kinase inhibitors. *Nat Chem Biol* 8, 982-989.